

# Undetectable Intracellular Free Copper: The Requirement of a Copper Chaperone for Superoxide Dismutase

T. D. Rae,<sup>1</sup> P. J. Schmidt,<sup>3</sup> R. A. Pufahl,<sup>1</sup> V. C. Culotta,<sup>3\*</sup>  
T. V. O'Halloran<sup>1,2\*</sup>

The copper chaperone for the superoxide dismutase (CCS) gene is necessary for expression of an active, copper-bound form of superoxide dismutase (SOD1) in vivo in spite of the high affinity of SOD1 for copper (dissociation constant = 6 fM) and the high intracellular concentrations of both SOD1 (10 μM in yeast) and copper (70 μM in yeast). In vitro studies demonstrated that purified Cu(I)-yCCS protein is sufficient for direct copper activation of apo-ySOD1 but is necessary only when the concentration of free copper ions ([Cu]<sub>free</sub>) is strictly limited. Moreover, the physiological requirement for yCCS in vivo was readily bypassed by elevated copper concentrations and abrogation of intracellular copper-scavenging systems such as the metallothioneins. This metallochaperone protein activates the target enzyme through direct insertion of the copper cofactor and apparently functions to protect the metal ion from binding to intracellular copper scavengers. These results indicate that intracellular [Cu]<sub>free</sub> is limited to less than one free copper ion per cell and suggest that a pool of free copper ions is not used in physiological activation of metalloenzymes.

Metalloproteins such as the antioxidant enzyme Cu,Zn-superoxide dismutase (SOD1) (1, 2) are generally assumed to acquire the essential cofactors by passive diffusion, although recent studies indicate that more complex mechanisms are involved. A network of copper-trafficking genes including *ATX1* and *LYS7* of *Saccharomyces cerevisiae* and their mammalian homologs are required for copper incorporation of proteins in vivo (3–7). The *LYS7* gene, which encodes the yeast copper chaperone for superoxide dismutase (yCCS) (4), is essential for expression of the functional, copper-bound form of yeast SOD1 (ySOD1) in vivo. Possible roles for yCCS in activation of ySOD1 include insertion of copper, stabilization of protein-folding intermediates, enhancement of protein stability, or modulation of intracellular copper availability in concert with other cellular factors. We found that yCCS directly inserts copper into the target enzyme and that this metallochaperone is necessary only if the ambient free copper concentration is exceedingly low. These results lead to the conclusion that the intracellular milieu has an extraordinary overcapacity for chelation of copper. In

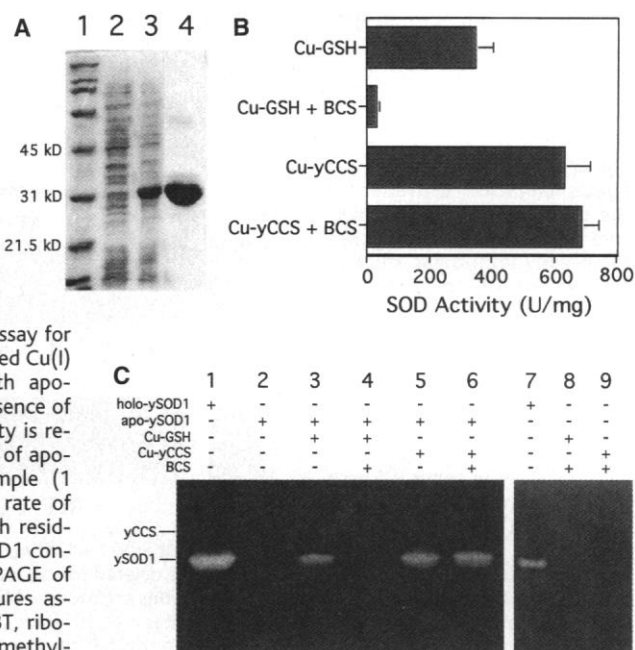
contrast to the emerging picture of energy-dependent iron uptake (8), we anticipate that this chelation capacity leads to a substantial driving force for copper passage into the cell.

The requirement for yCCS in vivo was first examined by measuring the intracellular concentrations of copper, yCCS protein, and

the ySOD1 target enzyme (9–12). In agreement with previous studies (4), we found that the absence of yCCS did not decrease the total number of ySOD1 molecules yet substantially reduced the ratio of the active, copper-bound ySOD1 to the inactive apo form of the enzyme (Table 1). In addition, the total number of copper atoms in these strains was similar regardless of the presence of yCCS or ySOD1 (Table 1), demonstrating that despite the loss of either abundant copper-binding protein, the number of copper ions per cell remains constant. Thus, there is no apparent role for yCCS in modulation of copper uptake or target enzyme stability.

To determine if this metallochaperone is sufficient for direct activation of the metal-depleted ySOD1 (apo-ySOD1), we expressed yCCS in *Escherichia coli*, purified it to homogeneity (Fig. 1A) (13), and incubated the copper-loaded form with purified samples of denatured apo-ySOD1 (14, 15). Yeast SOD1 enzyme was acid denatured and lyophilized after metal removal and was then treated with Cu(I)-yCCS or Cu(I)-GSH copper donors (Fig. 1, B and C). The glutathione (GSH) complex of Cu(I), a compound previously invoked as a possible physiological Cu donor (16), was used as a control. After incubation with copper donors, the resulting ySOD1 activity was assessed by the standard kinetic assay with cytochrome c (17). Apo-ySOD1 was activated upon treatment with either Cu(I)-yCCS or Cu(I)-GSH. Copper in either the cuprous [Cu(CH<sub>3</sub>CN)<sub>4</sub>PF<sub>6</sub>] or cupric (CuSO<sub>4</sub>) oxidation state also activated apo-ySOD1 under similar conditions. The yCCS metallochaperone is thus unnecessary for in

**Fig. 1.** In vitro analysis of yCCS metallochaperone function in activation of Cu,ZnSOD (ySOD1). (A) SDS-PAGE of the overexpression and purification of yCCS from *E. coli*. Lane 1, molecular size standards; lane 2, lysate from noninduced cells; lane 3, lysate from cells with yCCS protein induction; and lane 4, purified yCCS. (B) Cytochrome c-xanthine oxidase assay for SOD activity after the indicated Cu(I) sources were incubated with apo-ySOD1 in the presence or absence of the Cu(I) chelate, BCS. Activity is reported as units per milligram of apo-ySOD1 protein in each sample (1 U = 50% inhibition of the rate of cytochrome c reduction) with residual activity from an apo-ySOD1 control subtracted. (C) Native PAGE of the in vitro activation mixtures assayed in (B) stained with NBT, riboflavin, and *N,N,N',N'*-tetramethylethylenediamine for SOD activity. Amounts of ySOD1 protein applied to each lane are 40 and 20 ng of holo-ySOD1 in lanes 1 and 7, respectively, and 240 ng of apo-ySOD1 in each of lanes 2 to 6.



<sup>1</sup>Department of Chemistry and <sup>2</sup>Department of Biochemistry, Molecular Biology and Cell Biology, Northwestern University, Evanston, IL 60208, USA. <sup>3</sup>Department of Environmental Health Sciences, The Johns Hopkins University, Baltimore, MD 21205, USA.

\*To whom correspondence should be addressed. E-mail: vcullotta@jhsph.edu; t-ohalloran@nwu.edu

## REPORTS

**Table 1.** Amounts of copper and SOD1 per cell and resistance to copper toxicity in various yeast strains (9). Amounts of copper are reported in atoms per cell as determined by elemental analysis of whole cells (10). Total SOD1 and yCCS were determined by protein immunoblotting and are given as the number of molecules of monomers per cell (11). Active SOD1 is given as an upper limit of active SOD1 monomers per cell as determined by gel analysis of SOD1 activity (12). Mean inhibitory con-

centration (MIC) is the concentration of copper sulfate required to inhibit yeast growth in a synthetic dextrose minimal medium (27) by 50%. All measurements are given as a full range of values obtained over two to four independent samples except in the case of the copper determinations, where the uncertainty is the SD of two independent experiments of four measurements each. ND, not determined; null indicates total absence of protein due to gene deletion. WT, wild type.

Strain	Copper (atoms per cell)	Total SOD1 (monomers per cell)	yCCS (monomers per cell)	Active SOD1 (monomers per cell)	MIC <sub>Cu</sub> (μM)
SY1699 (WT)	$3.9 (\pm 0.2) \times 10^5$	$6.0 (\pm 2.0) \times 10^4$	$1.0 (\pm 0.2) \times 10^4$	$5.0 (\pm 3.0) \times 10^4$	740 (±100)
VC107 ( <i>sod1Δ</i> )	$3.0 (\pm 0.3) \times 10^5$	Null	$1.0 (\pm 0.3) \times 10^4$	Null	230 (±10)
SY2950 ( <i>lys7Δ</i> )	$2.3 (\pm 0.3) \times 10^5$	$5.0 (\pm 2.0) \times 10^4$	Null	$< 2 \times 10^2$	220 (±10)
VC279 ( <i>sod1Δ lys7Δ</i> )	ND	Null	Null	Null	190 (±10)

vitro ySOD1 activation if a sufficient pool of copper is accessible to the apo-enzyme.

In contrast, the *in vivo* measurements indicated that ySOD1 is inactive in the absence of yCCS, even though total cellular copper remains at normal concentrations (Table 1). The apparent disparity between *in vitro* and *in vivo* metal incorporation of ySOD1 is readily reconciled if the “free” copper concentration ( $[Cu]_{free}$ ) in the cytoplasm is strictly limited. In this model, yCCS functions both to sequester copper away from metal-scavenging agents and to direct the cofactor into the enzyme. To test this, we decreased  $[Cu]_{free}$  in the assay solutions by the addition of bathocuproine sulfonate (BCS), a chelating agent that reacts rapidly with and has high affinity for aqueous Cu(I) ions [dissociation constant ( $K_d$ )  $\sim 10^{-20}$  M] (18). With  $[Cu]_{free}$  minimized ( $\sim 10^{-17}$  M) by the presence of 0.2 mM BCS, Cu(I)-yCCS still activated the apo-enzyme, whereas activation by Cu(I)-GSH was nearly abolished (Fig. 1B). Similarly, activation by CuSO<sub>4</sub> donor was restricted with the addition of an appropriate Cu(II) chelate, such as EDTA ( $K_d = 1.6 \times 10^{-19}$  M). Thus, in the presence of copper-scavenging reagents, Cu(I)-CCS can activate ySOD1,

but Cu(I)-GSH and CuSO<sub>4</sub> cannot.

Samples of these same reconstitution mixtures were also assayed on native polyacrylamide gels stained for SOD activity with nitroblue tetrazolium (NBT) (Fig. 1C). The resulting SOD activity bands confirmed the previous conclusion and established that the bulk superoxide disproportionation activity detected in the kinetic assays arose from ySOD1 enzyme rather than other adventitious reactions. Control samples of Cu-yCCS or Cu-GSH that lacked apo-yCCS also displayed no SOD activity bands comparable to holo-ySOD1.

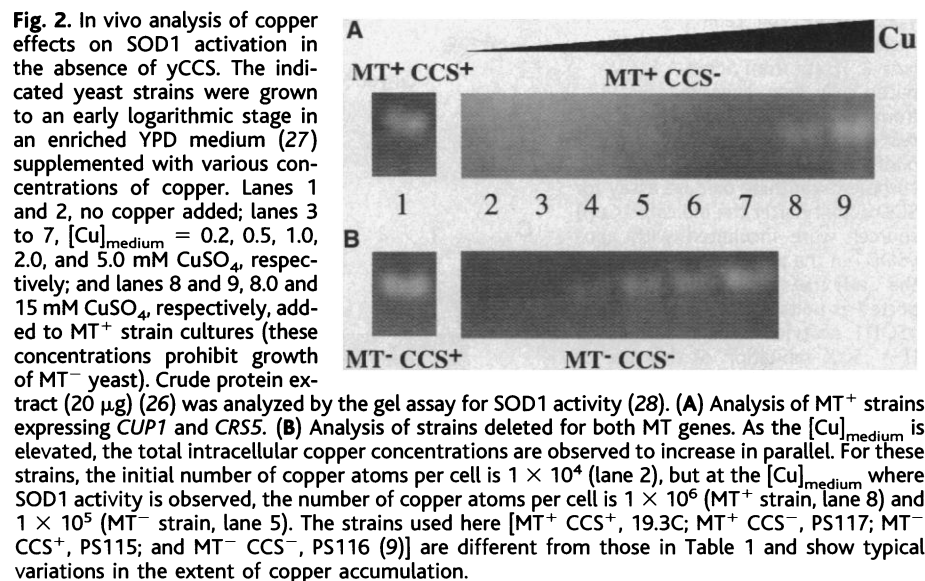
The *in vitro* results indicate that yCCS alone is sufficient for activation of the target enzyme. Furthermore, the metal insertion event apparently proceeds with direct transfer of the copper ion from yCCS to the ySOD1 target enzyme. The inability of Cu(I)-GSH to activate ySOD1 in the presence of BCS (Fig. 1B) precludes an indirect transfer mechanism in which copper is first released from yCCS into solution and subsequently binds to apo-SOD. Copper ions that may dissociate from yCCS or GSH are rapidly sequestered by the BCS competitor (present in 20-fold excess over the copper donor molecule), resulting in

a complex that is incapable of donating copper to ySOD1 apo-enzyme.

The biochemical activation data also suggest that the strict genetic requirement for yCCS will only be manifested when the cytoplasmic concentration of free copper is negligible. To test this proposition *in vivo*, we increased cytoplasmic concentrations of available copper by two means: exposure of cells to elevated copper concentrations in the growth medium ( $[Cu]_{medium}$ ) or elimination of cytoplasmic copper-sequestering proteins.

Elevation of  $[Cu]_{medium}$  from submicromolar concentrations to 5 mM failed to activate ySOD1 in cells lacking the yCCS metallochaperone. As  $[Cu]_{medium}$  was further increased to toxic amounts, however, the total number of copper atoms per cell increased by 100-fold and ySOD1 activity became apparent in native gels assays of cytoplasmic extracts (Fig. 2A). Thus, a key limitation to ySOD1 activity is the low availability of copper within the cell. Given that cells lacking the metallochaperone have similar amounts of copper and ySOD1 (Table 1) to wild-type cells, it is clear that the copper must be bound tightly at other sites that are inaccessible to apo-ySOD1. Candidates for such copper-sequestration sites include the yeast metallothionein isoforms encoded by *CUP1* and *CRS5* (19, 20).

The role of yeast metallothioneins in restricting intracellular  $[Cu]_{free}$  was evaluated in yeast strains with deleted *CUP1* and *CRS5* genes (designated MT<sup>-</sup>) that also lacked yCCS (9). In the absence of yCCS, ySOD1 activity in these strains was dependent on the dose of copper provided in the medium (Fig. 2B). ySOD1 activity became apparent at  $[Cu]_{medium} = 0.5$  mM, at which point cellular copper accumulation increased by 10-fold. This represents an order of magnitude less than the total cellular copper or  $[Cu]_{medium}$  required to activate a comparable amount of ySOD1 in the yeast strain expressing MTs (Fig. 2A). These results demonstrate that yeast metallothioneins limit copper availability to ySOD1. Because additional copper must still be added to the medium to observe SOD activity, MTs must provide only part of



the copper-chelation capacity in the cell. Furthermore, the fact that ySOD1 can be activated by copper in vivo in the absence of yCCS (Fig. 2) argues against an essential role for yCCS in activation of apo-ySOD1 through protein-folding pathways. We conclude that the yCCS molecule specifically delivers ~15% of the total cellular copper pool to saturate the ySOD1 pool (Table 1) in spite of an abundance of intracellular scavengers that maintain  $[Cu]_{free}$  at very low values.

The data in Table 1 are a reliable gauge for the number of relevant molecules per cell and provide a starting point for evaluating copper availability in the cell. Using these data and a thermodynamic model (21), we estimate the  $[Cu]_{free}$  in an unstressed cell to be less than in  $10^{-18}$  M. For comparison, one free copper atom in the same volume ( $10^{-14}$  liters) corresponds to a  $[Cu]_{free}$  of  $10^{-10}$  M. It is unclear whether the intracellular copper-ySOD1 system is at equilibrium; however, the rate of copper binding to ySOD1 in vitro is quite rapid (22). Using a kinetic model (22), we arrived at the same conclusion: There is less than one free copper atom per cell under normal growth conditions. Given the high intracellular capacity for copper binding, we anticipate that kinetic aspects of specific metallochaperone interactions will control the extent of copper transfer to target versus nontarget molecules.

The results indicate that intracellular copper availability is extraordinarily restricted. The extensive chelation capacity allows too few free copper ions to become available to saturate the 60,000 molecules of SOD1 within the typical life-span of a yeast cell. This provides a context for understanding the driving force for metal uptake in general (8) but more specifically underscores the physiological requirement for metallochaperones: Copper-dependent enzymes require accessory factors to compete with chelators and processes that sequester essentially all intracellular free copper. In this way, the metallochaperones protect copper ions. It has been suggested that copper chaperones protect cells against copper toxicity (3, 5). We do observe some protective effects of yCCS with respect to elevated  $[Cu]_{medium}$  (MIC values, Table 1), although this protection likely results from insertion of metal into ySOD1 (itself a cellular buffer for copper) rather than from sequestration by yCCS (23). The central function of this metallochaperone is to directly insert the cofactor into the target enzyme, thus converting the latter from an inactive to an active state. In this sense, the function of the yCCS protein is analogous to that of the molecular chaperones, although it is unclear at this time whether yCCS also increases the efficiency of ySOD1 folding. These issues may be important in understanding the pathological features of the large number of known

mutations in human SOD1 that lead to amyotrophic lateral sclerosis (24, 25).

*Note added in proof:* Since submission of this paper, Lyons *et al.* (31) have proposed that in the absence of yCCS, intracellular SOD1 exists with one zinc ion bound per SOD dimer. This is compatible with our results, which do not address whether zinc is bound by SOD1 before or after copper insertion by yCCS.

References and Notes

1. I. Bertini, S. Mangani, M. S. Viezzoli, *Adv. Inorg. Chem.* **45**, 127 (1998).
2. J. S. Valentine and M. W. Pantoliano, in *Copper Proteins*, T. G. Spiro, Ed. (Wiley, New York, 1982), pp. 292–358.
3. R. A. Pufahl *et al.*, *Science* **278**, 853 (1997).
4. V. C. Culotta *et al.*, *J. Biol. Chem.* **272**, 23469 (1997).
5. J. S. Valentine and E. B. Gralla, *Science* **278**, 817 (1997).
6. S.-J. Lin *et al.*, *J. Biol. Chem.* **272**, 9215 (1997).
7. R. L. B. Casareno *et al.*, *ibid.* **237**, 23625 (1998).
8. D. Radisky and J. Kaplan, *ibid.* **274**, 4481 (1999).
9. The isogenic wild-type SY1699 and *lys7* null SY2950 strains were described [J. Horecka, P. T. Kinsey, G. F. Sprague, *Gene* **162**, 87 (1995)]. VC107 and VC279 are *sod1Δ::TRP1* derivatives of SY1699 and SY2950. PS115 is an *Ura<sup>+</sup>* derivative of 51-2C (*cup1Δ crs5Δ*) (20) obtained by selection on 5-FOA [J. Boeke, F. LaCroute, G. Fink, *Mol. Gen. Genet.* **197**, 345 (1984)]. PS116 and PS117 were created by deleting the *LYS7* gene of PS115 and the congenic wild-type 19.3C strain (*CUP1<sup>+</sup> CRS5*) with a *lys7Δ::URA3* disruption plasmid (P. J. Schmidt and V. C. Culotta, unpublished data).
10. Milli-Q water was treated with Chelex 100 (Bio-Rad) to remove trace metals. Yeast cells were dried overnight at 75° to 80°C until no further change in mass was observed, dissolved in concentrated nitric acid (300 to 500 μl), and heated at 80°C for 30 min. Parallel control experiments examined background amounts of copper in the materials used. Elemental analysis of hydrolyzed cells was measured by inductively coupled plasma-atomic emission spectroscopy (AtomScan ICP-AES).
11. The amounts of ySOD1 and yCCS were measured in whole-cell extracts (26) prepared from cells grown to an early logarithmic phase in enriched yeast extract, peptone, and dextrose (YPD) medium (27). Protein immunoblotting was done with 1 to 200 ng of purified yCCS or purified ySOD1 as standards (*vida infra*) and detected with polyclonal rabbit antisera to yCCS (Biodesign International, Kennebunk, ME) or yeast SOD1. We observed that 15 μg of the extract protein (corresponding to  $5.35 \times 10^6$  yeast cells on the basis of our empirical estimations of 2.8 pg of protein yield per cell for strain SY1699) contained 9 to 10.5 ng of SOD1 or 2 to 3 ng of yCCS, corresponding to about  $6 \times 10^4$  and  $1 \times 10^4$  molecules per cell, respectively.
12. To determine the number of copper-loaded SOD1 molecules per cell, crude yeast extract protein [prepared as described (17) and concentrated as needed] was subjected to a nondenaturing gel-NBT assay for SOD1 activity (28). Purified ySOD1 (14) was used as a standard and was shown to be fully loaded with copper by elemental analysis. The lower limit of detection was 2 ng ( $7.6 \times 10^{10}$  monomers) of copper-loaded SOD1. SOD1 from wild-type strains exhibited 50 to 100% of the activity of the ySOD1 standard, whereas no SOD1 activity could be detected in *lys7* null strains, even in samples containing  $3.0 \times 10^8$  cells.
13. The *LYS7* gene was amplified by polymerase chain reaction, subcloned into pET11d (Novagen), and confirmed by restriction mapping and DNA sequencing. In this process, the second amino acid was altered from Thr to Ala. Constructs were transformed into *E. coli* strain BL21(DE3) for overexpression. yCCS was purified by chromatography on anion exchange, cation exchange, and size exclusion resins. Electrospray

mass spectrometry (ESI-MS) gave a single peak at mass-to-charge ratio  $m/z = 27,169$  daltons, which agrees with the predicted molecular mass of the full-length protein minus the  $NH_2$ -terminal methionine. Protein concentrations were determined with a calibrated Bradford (Bio-Rad) curve with immunoglobulin G as the standard. A correction factor of 2.28 was necessary to correct the overestimation of yCCS by the Bradford method as determined by amino acid hydrolysis. The Cu(I) complex of yCCS was obtained by incubation of purified yCCS (100 μM) in 50 mM tris (pH 8.0), 10 mM dithiothreitol (DTT), and 200 mM NaCl with 1 molar equivalent of Cu(I)(CH<sub>3</sub>CN)<sub>4</sub>PF<sub>6</sub> complex for 2 hours. Cu(I)-yCCS was then washed with repeated dialysis with the same tris/DTT/NaCl buffer, followed by dialysis exchanges against 50 mM tris (pH 8.0) alone to remove DTT and NaCl. All stages of the Cu(I)-yCCS complexation procedure were performed in an anaerobic glove box. Copper analysis by ICP-AES and calibrated Bradford protein assay revealed a 1.1:1 Cu(I)-yCCS complex.

14. Yeast SOD1 protein for activation assays was expressed in *E. coli* BL21(DE3) transformed with ySOD1-pET3d and isolated by anion exchange chromatography. Isolated enzyme was then denatured and demetallated by treatment with 0.1 M DTT, 10 mM EDTA, 1 mM BCS, 15% CH<sub>3</sub>CN, and 0.1% trifluoroacetic acid, followed by further purification by reverse-phase high-performance liquid chromatography through a C4 Vydac 214TP54 column. The ySOD1 protein fractions were combined, dried under vacuum, and applied directly to the in vitro activation assays described below. A mass of 15,722.5 daltons determined by ESI-MS confirmed the identity of the purified ySOD1 monomer (theoretical mass of 15,723 daltons). Holo-ySOD1 for positive controls was isolated from baker's yeast cake by the chloroform-ethanol extraction procedure as described (29).
15. All samples for activation assays contained 1.8 μM apo-ySOD1, 1 mM GSH, and 20 μM ZnSO<sub>4</sub> in 50 mM potassium phosphate buffer (pH 7.8). Where indicated in Fig. 1, specific reaction mixtures included either 10 μM Cu(I)-yCCS or 10 μM Cu(I)(CH<sub>3</sub>CN)<sub>4</sub>PF<sub>6</sub> and 0 or 200 μM BCS. The standard cytochrome c-xanthine oxidase assay for SOD activity (17) was executed in triplicate for each reaction mixture, and 1 mM EDTA was included in the assay buffer. SOD activity staining of native polyacrylamide gel electrophoresis (PAGE) gels with NBT was done as described (28). Native PAGE of in vitro activation mixtures contained 0.1 mM EDTA in the running buffer.
16. M. R. Ciriolo, A. Desideri, M. Paci, G. Rotilio, *J. Biol. Chem.* **265**, 11030 (1990).
17. I. Fridovich, in *CRC Handbook of Methods for Oxygen Radical Research*, R. A. Greenwald, Ed. (CRC Press, Boca Raton, FL, 1985), pp. 213–215.
18. The stability constant for Cu(I)(BCS)<sub>2</sub> is not available. The value for the closely related *bis*-(2,9-dimethyl-1,10-phenanthroline)copper(I) complex,  $\log(\beta_2) = 19.1$ , was used [C. J. Hawkins and D. D. Perrin, *J. Chem. Soc.* **1963**, 2996 (1963)].
19. M. Karin *et al.*, *Proc. Natl. Acad. Sci. U.S.A.* **81**, 337 (1984).
20. V. C. Culotta *et al.*, *J. Biol. Chem.* **269**, 25295 (1994).
21. The number of active SOD1 molecules in a *lys7* null strain grown under normal conditions cannot be greater than 200 of the 50,000 SOD monomers per cell (Table 1), based on the 2-ng detection limit for staining of SOD activity on native gels (12). Applying the conditional equilibrium constant expression for Cu(II) binding to bSOD1



$$[Cu(II)]_{free} = [Cu-SOD]/K_1'[apo-SOD] = f/K_1'(1-f) \quad (2)$$

where  $K_1'$  [the association constant for the first Cu(II) binding at pH = 7.0] is  $4 \times 10^{15} M^{-1}$  (30), and our measurement of the fraction of Cu-SOD in the cell (where  $f = [CuSOD]/[SOD]_{total} < 200/50,000$ ), an upper limit for the magnitude of the free copper concentration available to apo-SOD is calculated as  $[Cu]_{free} < 10^{-18} M$ . This value does not require an estimate of the volume accessible to diffusing reactants within the cell. Although measured values for  $K_1'$  are reported from  $10^{14}$  to  $10^{17} M^{-1}$  at pH values between 7 and 10, a variance of several orders of

magnitude in this parameter does not alter our conclusion that cells typically maintain free copper at insignificant concentrations. The upper limit for  $[Cu(I)]_{free}$  calculated in the same manner as for  $Cu(II)$ , is estimated to be less than  $10^{-23}$  M. To obtain this value, we used the known  $Cu(I)/Cu(II)$  reduction potentials of CuSOD (400 mV) and aqueous  $Cu(II)$  (153 mV) in a thermodynamic cycle with the  $K_1'$  of Eq. 1 to obtain an equilibrium constant for  $Cu(I)$  binding to SOD ( $2 \times 10^{20}$ ). The equilibrium  $[Cu(I)]_{free}$  would be five orders of magnitude lower than estimates for  $Cu(II)$ .

22. A less reliable kinetic model yields a range of intracellular  $[Cu]_{free}$  values for the *lys7* null strain data in Table 1. Assumptions include a second-order rate law  $d[CuSOD]/dt = k_1 [apo-SOD][Cu]_{free}$  where  $[apo-SOD] \sim 10 \mu M$  (moles of total SOD1 per volume of a cell),  $t$  is time, and  $k_1$  is the second-order rate constant. The rate  $d[CuSOD]/dt < 3 \times 10^{-8}$  M per 60 hours is about  $10^{-13} M s^{-1}$ , where 60 hours corresponds to the typical lifetime of a yeast cell with a doubling time of  $\geq 2$  hours and a life-span of no more than 30 divisions [D. A. Sinclair, K. Mills, L. Guarente, *Trends Biochem. Sci.* **23**, 131 (1998)]. The volume accessible to ySOD and copper

ions is assumed to be about 1/4 of the total volume of a yeast cell, where the latter is  $7 \times 10^{-14}$  liters [F. Sherman, in *Methods in Enzymology*, C. Guthrie and G. R. Fink, Eds. (Academic Press, Orlando, FL, 1991), vol. 194, pp. 3–21]. Two limiting conditions for  $k_1$  were considered. If the rate for copper binding to ySOD1 is diffusion controlled ( $k_1 = 10^8 M^{-1} s^{-1}$ ), the upper limit of  $[Cu]_{free}$  is  $10^{-16}$  M. When a lower limit for  $k_1$  of  $10^4 M^{-1} s^{-1}$  was used,  $[Cu]_{free}$  is  $< 10^{-12}$  M. This lower limit for  $k_1$  was obtained by measuring the increase in active ySOD1 concentration (by cytochrome *c* assay) after incubation of  $Cu(II)$  with apo-ySOD1 for 5 to 60 s. Metal insertion was quenched by EDTA (1 mM), which prevents further loading of apo-ySOD1.

23. V. C. Culotta *et al.*, *J. Biol. Chem.* **270**, 29991 (1995).  
 24. D. R. Rosen *et al.*, *Nature* **362**, 59 (1993).  
 25. H.-X. Deng *et al.*, *Science* **261**, 1047 (1993).  
 26. S.-J. Lin and V. C. Culotta, *Mol. Cell. Biol.* **16**, 6303 (1996).  
 27. F. Sherman *et al.*, *Methods in Yeast Genetics* (Cold Spring Harbor Laboratory Press, Cold Spring Harbor, NY, 1978).  
 28. L. Flohe and F. Otting, in *Methods in Enzymology*, L.

- Packer, S. P. Colowick, N. O. Kaplan, Eds. (Academic Press, Orlando, FL, 1984), vol. 105, pp. 93–104.  
 29. S. A. Goscin and I. Fridovich, *Biochim. Biophys. Acta* **289**, 276 (1972).  
 30. J. Hirose, T. Ohhira, H. Hirata, Y. Kidani, *Arch. Biochem. Biophys.* **218**, 179 (1982).  
 31. T. J. Lyons *et al.*, *J. Biol. Inorg. Chem.* **3**, 650 (1998).  
 32. We thank D. Hamer for yeast strain 19.3C; J. Valentine for the ySOD1-pET3d plasmid; D. Kosman for yeast SOD1 antibody; I. Klotz, J. Widom, and D. Huffman for advice; and J. Strain, A. Torres, and A. Herrreiter for technical assistance. Supported in part by NIH grants GM 54111 (T.V.O.), GM 50016 (V.C.C.), F32 GM19457 (T.D.R.), and F32 DK09305 (R.A.P.); National Institute of Environmental Health Science training grant ES07141 (P.J.S.); the Johns Hopkins University National Institute for Environmental Health Science Center (V.C.C.); and the Amyotrophic Lateral Sclerosis Association (T.V.O.). T.V.O. is a member of the Robert H. Lurie Comprehensive Cancer Center.

28 December 1998; accepted 18 March 1999

## Effects of Angiogenesis Inhibitors on Multistage Carcinogenesis in Mice

Gabriele Bergers,<sup>1</sup> Kashi Javaherian,<sup>2</sup> Kin-Ming Lo,<sup>3</sup> Judah Folkman,<sup>2</sup> Douglas Hanahan<sup>1\*</sup>

Solid tumors depend on angiogenesis for their growth. In a transgenic mouse model of pancreatic islet cell carcinogenesis (RIP1-Tag2), an angiogenic switch occurs in premalignant lesions, and angiogenesis persists during progression to expansive solid tumors and invasive carcinomas. RIP1-Tag2 mice were treated so as to compare the effects of four angiogenesis inhibitors at three distinct stages of disease progression. AGM-1470, angiostatin, BB-94, and endostatin each produced distinct efficacy profiles in trials aimed at preventing the angiogenic switch in premalignant lesions, intervening in the rapid expansion of small tumors, or inducing the regression of large end-stage cancers. Thus, anti-angiogenic drugs may prove most efficacious when they are targeted to specific stages of cancer.

Over the past decade, genetically engineered mouse models of cancer have increasingly been used in studies on mechanisms of carcinogenesis. One strength of these models is that cancers arise from normal cells in their natural tissue microenvironments and progress through multiple stages, as does human cancer (1). Such models of organ-specific cancer also present opportunities for development not only of cancer therapies but also of preventative strategies that block the progression of premalignant lesions into tumors.

The RIP1-Tag2 transgenic mouse model

of pancreatic islet carcinogenesis serves as a general prototype of the pathways, parameters, and molecular mechanisms of multistage tumorigenesis. The pathway through which normal insulin-producing  $\beta$  cells of the pancreatic islets are converted into islet cell carcinomas under the influence of the SV40 T antigen (Tag) is increasingly well understood (2, 3). Briefly, in the RIP1-Tag2 line, the following stages arise sequentially over the 13.5-week average lifetime of these mice. Normal islets (initially 100% of the  $\sim 400$  islets per pancreas) express the Tag oncogene and yet are morphologically asymptomatic until 3 to 4 weeks of age. Hyperplastic islets then begin to appear stochastically (increasing to 50% of the islets by 10 weeks), displaying  $\beta$ -cell hyperproliferation and features of dysplasia and carcinoma in situ. Angiogenic islets (8 to 12%) arise from hyperplastic/dysplastic islets by switching on angiogenesis in the normally quiescent islet capillaries (3). This switch is characterized by

endothelial proliferation, vascular dilation, and microhemorrhaging. Solid tumors ( $\sim 3\%$  of the islets) emerge at 10 weeks as small encapsulated tumors (adenomas) that progress by 12 to 13 weeks into large adenomas and (less frequently) invasive carcinomas, both of which are intensely vascularized by dilated hemorrhagic vessels.

In earlier work, we showed that a mixture of three angiogenesis inhibitors (AGM-1470, minocycline, and alpha interferon) could inhibit tumor growth in the RIP-Tag model (4). These data supported other preclinical data from subcutaneous transplant models (5–7). Encouraged by the result, we designed the present study to assess the effects of four diverse angiogenesis inhibitors when applied to RIP1-Tag2 mice at three distinct stages of pancreatic islet carcinogenesis. Figure 1 illustrates the experimental design, which had three branches: (i) early treatment at the hyperplastic stage to block the angiogenic switch before the initial formation of solid tumors (prevention trial), (ii) treatment of mice bearing small (asymptomatic) solid tumors to determine whether their expansive growth and progression to deleterious stages could be stopped (intervention trial), and (iii) treatment of mice with substantial tumor burden and near death to ascertain whether these agents could induce tumor regression (regression trial). We evaluated four angiogenesis inhibitors (8) (Tables 1 and 2): AGM-1470 (TNP470), BB-94 (batimastat), angiostatin, and endostatin, as well as the combination of angiostatin and endostatin. AGM-1470 (TNP470) is a small molecule inhibitor of endothelial cell proliferation (9) that is thought to act by inhibiting an intracellular enzyme, methionylaminopeptidase-2 (9). BB-94 (batimastat) is a broad-spectrum inhibitor of matrix metalloproteinases (10), which are involved in the remodeling of extracellular matrix and capillary basement membranes during angiogenesis (11). An-

<sup>1</sup>Department of Biochemistry and Biophysics and Hormone Research Institute, University of California, San Francisco, 513 Parnassus Ave, San Francisco, CA 94143-0534, USA. <sup>2</sup>Department of Surgery, Children's Hospital Medical Center and Harvard Medical School, 300 Longwood Avenue, Boston, MA 02115, USA. <sup>3</sup>Lexigen Pharmaceuticals, 125 Hartwell Avenue, Lexington, MA 02173, USA.

\*To whom correspondence should be addressed. E-mail: dh@biochem.ucsf.edu